International Journal of Engineering Science Invention (IJESI)
ISSN (Online): 2319 – 6734, ISSN (Print): 2319 – 6726
www.ijesi.org ||Volume 7 Issue 3 Ver. I || March 2018 || PP. 12-18

An Efficient and Enhanced Photo catalytic Activity of Zno Nano particles on Mineralization of Congo red Dye in Aqueous Medium

T. Jeyapaul[1], S.Harikengaram[2], A.Chellamani[3]
[1]*Department of Chemistry, The MDT Hindu College, Tirunelveli,Tamilnadu, India*
[2]*Department of Chemistry, PMT College, Tirunelveli, Tamilnadu, India*
[3]*Department of Chemistry, Manonmaniam Sundharnar University, Tirunelveli, Tamilnadu, India*
Corresponding Author: T. Jeyapaul

ABSTRACT: *ZnO microspheres were successfully synthesized by a wet chemical method. The structure and morphology of the samples were investigated by X-ray diffraction and Scanning electron microscopy. X-ray diffraction revealed the hexagonal structure of ZnO. Percentage of lattice contraction and average particle size of the sample were also calculated from the XRD. SEM micrographs showed the spherical shape of ZnO nanoparticles. The UV-VIS absorption spectra showed red shift in wavelength corresponding to bulk. Photo degradation of congo red were investigated using ZnO microspheres. Among all, ZnO synthesized at 45mM concentration of ammonia added showed excellent photocatalytic activity to dye, which can be attributed to the improved charge separation. Since this process does not require any oxidants and uses the solar and UV light, it can be developed as an economically feasible and environmentally friendly method to decolorize for the wastewater treatment under sunlight*.

KEYWORDS: *ZnO nanoparticles, SEM, XRD, UV-Vis spectroscopy, photocatalyst.*

Date of Submission: 16-02-2018 Date of acceptance: 03-03-2018

I. Introduction

Oxide semiconductors have attracted a large amount of attention due to their potential application in the areas of catalysis, sensors, optics and solar cells [1, 2]. Among the metal oxides ZnO is a potential semiconductor with direct wide band gap (3.37 eV), has received enormous scientific attention because of its promising applications of optoelectronic nano-devices, piezoelectric nano-generators, dye-sensitized solar cells, biodevices and photocatalysts for degradation and complete elimination of environmental pollutants [3-6]. ZnO reveals the promising photo catalytic efficiency. The photocatalytic activity of ZnO has been improved by various techniques such as modification of ZnO by preparative methods, non-metal doping, and addition of transition metals as well as use of coupled semiconductors [7]. Modifying the preparative methods can reduce the band gap, extending the absorbance range to visible light region leading to electron–hole pair separation under irradiation and consequently, achieving a higher photocatalytic activity [8-10]. The ZnO nanoparticles can be prepared on a large scale at low cost by simple solution - based methods, such as chemical precipitation method. Numerous methods have been reported in the preparation so far, there are very few reports are there by changing the concentration of base in the chemical precipitation method.

Herein we reported that ZnO nanoparticles by novel chemical method using stable, less toxic inorganic salts as the reactants. The synthesized ZnO particles have been characterized using X-ray diffraction (XRD), scanning electron microscopy (SEM) and UV-Vis spectroscopy respectively. The photocatalytic activities in the degradation of congo red (CR) dye have been investigated in detail for the first time to the best of authors.

II. Experimental

1. Preparation of photocatalyst:

The zinc oxide (ZnO) nanoparticles were prepared by chemical method [11] using zinc acetate dihydrate and ammonia as precursors. Zinc acetate dihydrate (15mM) and different concentrations of liquid ammonia (30mM, 45mM and 60mM) were made up with 200 ml of distilled water was added dropwise in the above solution. Then the solution was kept under constant stirring using magnetic stirrer to completely dissolve the zinc acetate for 2 hour at 55 ºC. After the completion of reaction, the solution was allowed to settle for overnight and the supernatant solution was then discarded carefully. The remaining solution was centrifuged for 10 min and the supernatant was discarded. Thus obtained nanoparticles were washed three times using distilled water, ethanol and acetone. Washing was carried out to remove the byproducts that were bound with the nanoparticles. After washing, the nanoparticles were dried at room temperature for overnight. During drying,

complete conversion of zinc hydroxide into zinc oxide takes place. Resulting sample has annealed at 250 ºC for 2 hours.

2.2 Test of photocatalytic activity:

The photocatalytic activity was evaluated by employing a multiwavelength multilamp photo reactor fitted with 8W mercury lamps of wavelengths 365nm, 312nm and 254nm (Heber, Chennai) and a highly polished anodized aluminum reflector. A borosilicate glass tube of 15 mm inner diameter was used as the reaction vessel for the 365nm wavelength region, in case of 312nm and 254nm wavelength region quartz glass tube was used as the reaction vessel and was placed at the center of the reactor. The cooling fans at the bottom of the reactor dissipate the generated heat. The reactor was illuminated with eight lamps mutually set at right angle. The photon flux (I) of the UV light was determined by ferri oxalate actinometry.

A 50 mg of catalyst was added to the 75 ml of the CR dye solution in a 150 ml reaction vessel. At given time intervals, 5ml of aliquots were collected. The degraded solutions were analyzed using the absorption peaks at 488 nm. After the degradation the catalyst was separated from the reaction mixture and dried to carry out the reusability tests. The procedure of degradation of other dyes was similar to that of CR. Prior to irradiation, the suspensions were magnetically stirred in the dark for 20 min to ensure the equilibrium of the working solution.

III. Results And Discussion

The X-ray diffraction data were recorded by using Cu Kα radiation (1.5406 Aº). The intensity data were collected over a 2θ range of 10-80º. The average grain size of the samples was estimated with the help of Scherrer equation using the diffraction intensity of (101) peak. X-ray diffraction studies confirmed that the synthesized materials were ZnO with hexagonal phase and all the diffraction peaks agreed with the reported JCPDS data [12] and no characteristic peaks were observed other than ZnO. The mean crystallite size (D) of the particles was determined from the XRD line broadening measurement using Scherrer equation [13]. A definite line broadening of the diffraction peaks is an indication that the synthesized materials are in nanometer range. The grain size was found to be in the range of 9-17 nm depending on the growth condition. The lattice parameters calculated were also in agreement with the reported values. All the peaks match well with the standard cubic structure [14] and the FWHM of the (101) diffraction peak decreases with the increasing concentration of the NH_3. These results reveal that the molar ratio of OH^- to Zn^{2+} is a dominant factor for the formation of the ZnO nanoparticles.

With increasing ammonia concentration from 30 mM to 60 mM peak height increases and FWHM increases as result diffraction peaks become stronger and sharper, thereby indicating that the crystal quality has been improved and the size of particles become bigger. With increasing ammonia concentration, the crystallinity of the particles increases causing particles become bigger. Thus, in order to get smaller particles lower ammonia concentration is favourable.

$$Zn(CH_3COO)_2 + 2NH_4OH \rightleftharpoons Zn(OH)_2 + 2CH_3COONH_4$$

$$Zn(OH)_2 \rightarrow ZnO + H_2O$$

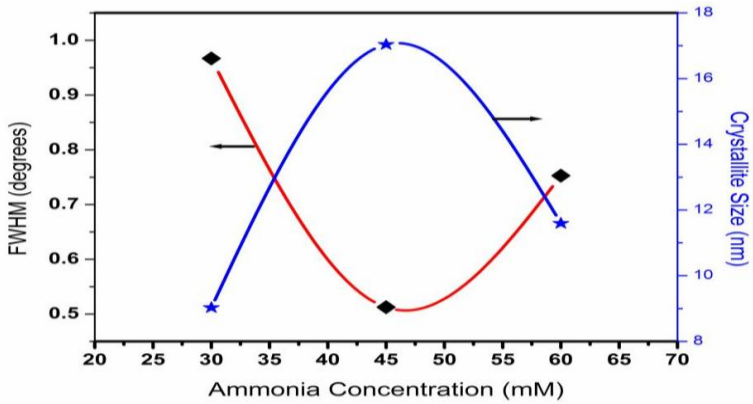

Figure 1. The variation of FWHM and Crystallite size of ZnO nano particle with various concentration of ammonia

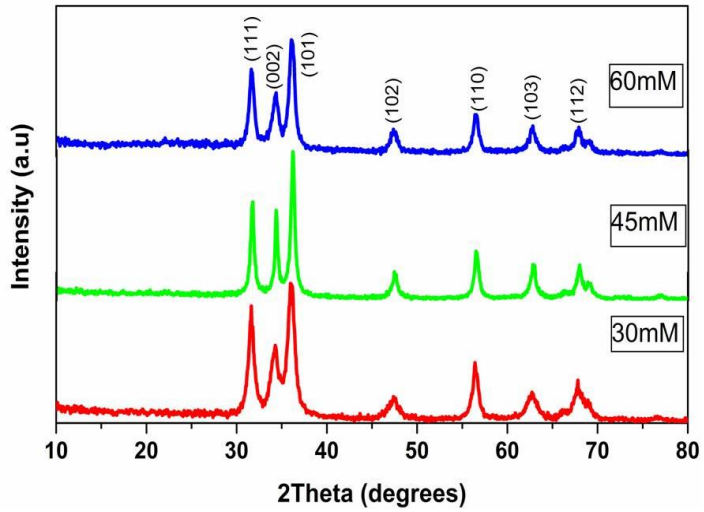

Figure 2. XRD pattern of ZnO nanoparticles synthesized from various concentration of ammonia

Zinc oxide nano particles were synthesized and it was characterized by the scanning electron microscope. The surface morphology of the nanoparticles was examined by using Scanning Electron Microscope (SEM). The SEM photographs are as shown in the Figure.3 a, b & c which demonstrates clearly the formation of zinc oxide nanoparticles and in various sizes. The nanoparticles were spherical in shape. The micrographs are shown below figure. 3(a) shows that a network formation of the ZnO has taken place. It clearly indicates that agglomeration has taken place. Similarly, in figure.3 (b) a big aggregation of the sample ZnO particles have been taken place. It is not possible to predict the exact size of the individual particle. SEM was used for microstructure study to find agglomeration. Nucleation and growth rate increases with increase ammonia concentration, as a result agglomeration is more in the sample concentration of 45 mM.

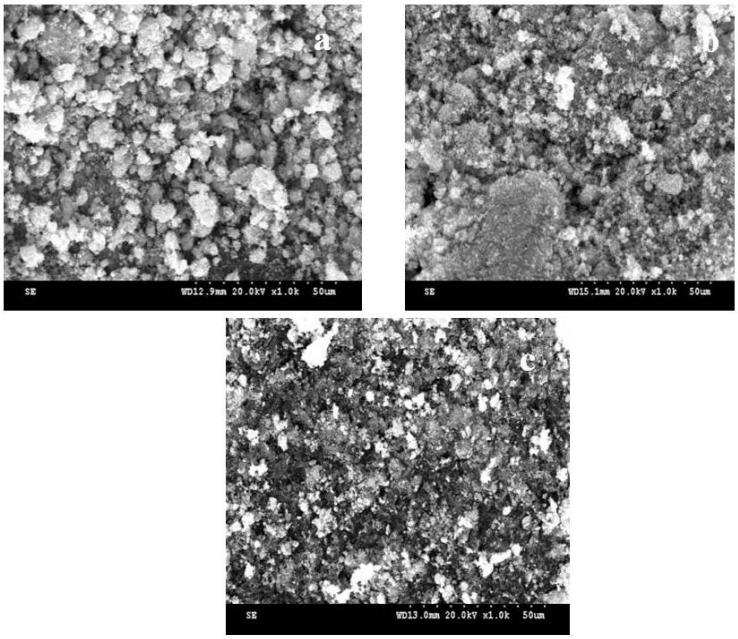

Figure 3. The SEM images ZnO nanoparticle with various concentration of ammonia (a) 30mM (b) 45mM (c) 60mM

The ZnO nanoparticles exhibit an increase in UV absorption and a slight increase in visible wavelength absorption. The absorption spectra shows the cut-off wavelengths for both samples to be around 375 nm, a 5 nm blue shift compared with the bulk material (380 nm).

Figure 4 shows the absorbance spectrum of ZnO nanoparticles at ammonia concentrations. Typical exciton absorption at 409 nm is observed in the absorption spectrum 60 mM, which is red shifted with respect to the bulk absorption edge appearing at 375nm. It is clear that the absorption edge systematically shifts to the longer wavelength. This pronounced and systematic shift in the absorption edge is due to the quantum size effect [15, 16].

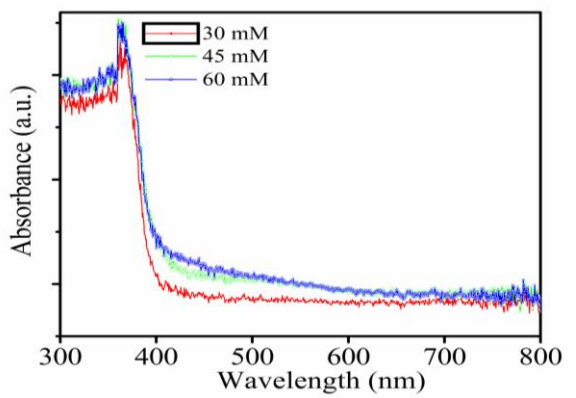

Figure 4. The absorbance spectra of ZnO nanoparticle with various concentration of Ammonia (a) 30mM (b) 45mM (c) 60mM

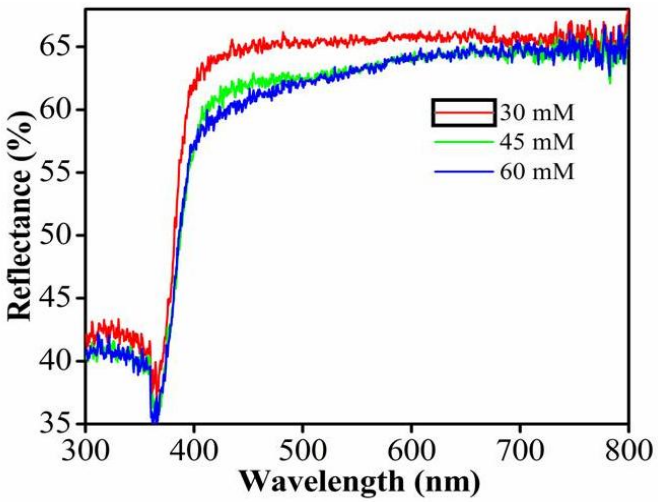

Figure 5. The UV-Vis reflectance spectra of ZnO nanoparticle with various concentration of ammonia (a) 30mM (b) 45mM (c) 60mM

Figure 5 represents the UV-Vis reflectance spectrum of ZnO nanoparticles. From which, we can calculate the band gap energy using Tauc relation. UV-Vis reflectance spectrum has less effect in scattering than absorption. The sudden decrease of reflectance at a particular wavelength, corresponding to the optical band gap means that the particles are almost uniformly distributed in the sample.

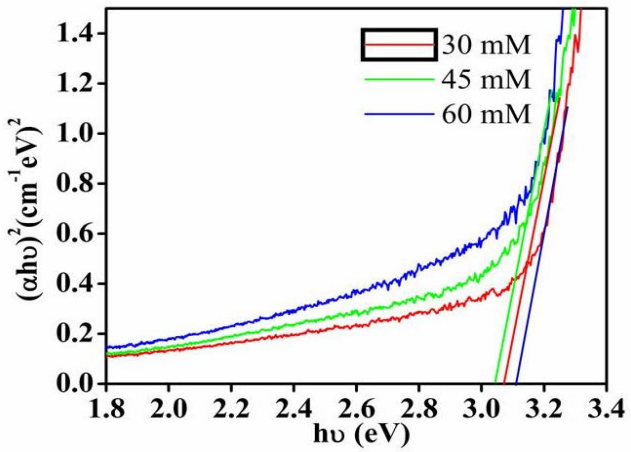

Figure 6. The energy bandgap diagram of ZnO nanoparticle with various concentration of Ammonia (a) 30 mM (b) 45 mM (c) 60 mM

Figure 6 represents the energy bandgap diagram of ZnO nanoparticle with various ammonia concentrations. The energy bandgap value is higher than that of 3.3 eV reported in the literature [17]. The band

gap of the ZnO nanopaticle synthesized in different ammonia concentration are found to be in the range between 3.04 -3.1 eV. Band gap energy decreases with increasing ammonia concentration due to quantum size effects.

The UV light photocatalytic tests of ZnO microspheres were evaluated by degradation of CR aqueous solution under UV light irradiation. The photocatalytic degradation of CR is showed in Figure 7. The C/C_0 (where C was the main absorption peak intensity of CR sampled at each irradiated time interval at a wavelength of 488 nm and 339nm, and C_0 was the absorption intensity of initial 10ppm CR solution) was plotted against the wavelength. There was almost no decolourization in the solution without any catalysts and also with catalyst in the dark. There is no adsorption of dye in the catalyst was detected. The colour of the dispersion solution disappeared after 25mins. From the Figure 7, it can be seen that after 25min of irradiation the main absorption peak of CR (λ) 488 nm nearly 90% disappeared, and the other small peaks decreased, too.

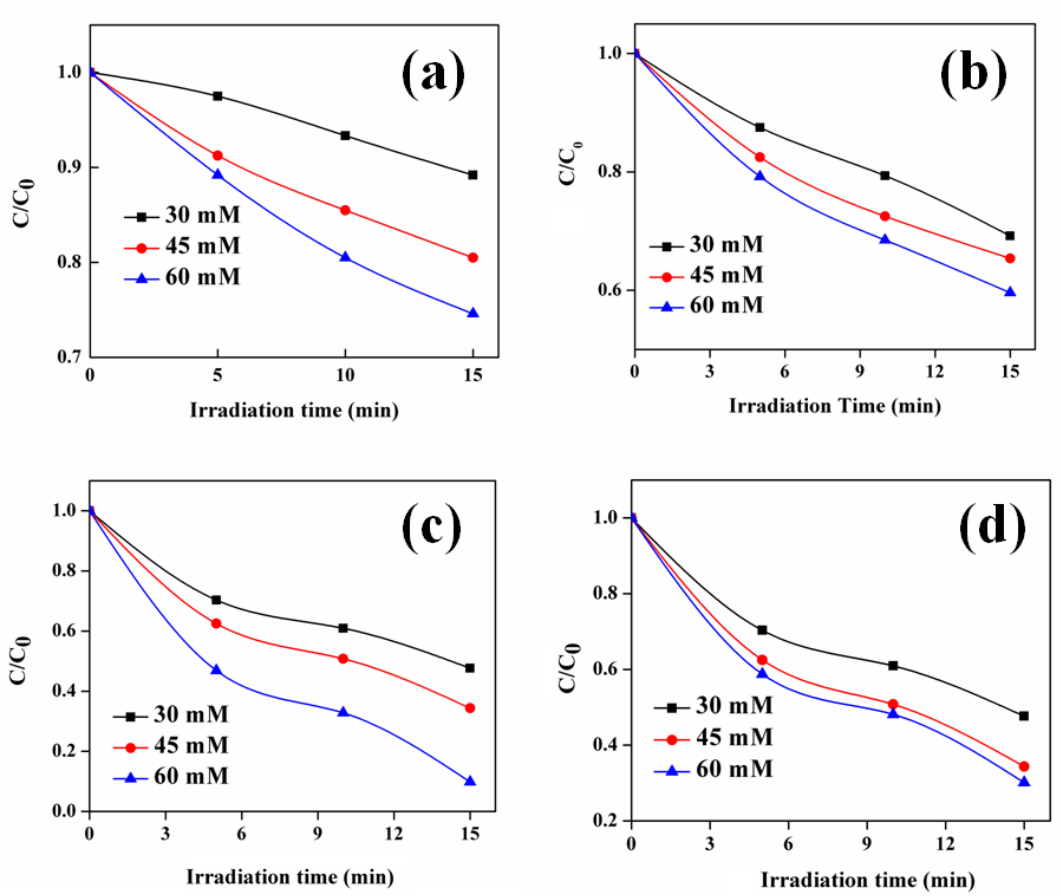

Figure 7. Photo degradation of CR under different light intensity (a) 2 lamp, (b) 4 lamp, (c) 6 lamp, (d) 8 lamp.

3.1 Physicochemical factors that influences the dye degradation:

This section examines the effects of various physicochemical parameters including light intensity, initial dye concentration, and amount of catalyst on the degradation of the dye after UV-Vis illumination for different lengths of time.

The effects of changes in the photo illumination intensity on the dye degradation were studied by varying the light intensity between 16W/cm^{-2} to 64W/cm^{-2}. Figure 7 shows that the conversion of the dye under various light intensities. The dye conversion increases when the light intensity increases from 16 to 64 W/cm^{-2}. It is also observed that the dye conversion remained almost constant at higher light intensities. The dye degradation increases from 0.1 to 0.06 as the light intensity increases from 16 and 64 W/cm^{-2}. At lower light intensities, the incident photon flux on the ZnO surface is not sufficient to excite all the available electron-hole pairs. This implies that too few electron-hole pairs are generated and hence limited holes are available to assist in the photo-oxidation of CR. An increase in light intensity leads to the generation of more electron-hole pairs which contributes to the formation of oxidizing species in greater concentrations.

Although an increase in light intensity from 16 to 48 W/cm^{-2} increases the degradation of CR, further increases in the light intensity beyond this point result in no significant increase in degradation. Similar results have been observed with different textile dyes [18, 19]. Such observations can be attributed to either increased

electron-hole recombination and/or absence of species to scavenge the photo generated holes. Primarily, greater electron-hole pair recombination rates at higher light intensities limits fractional conversion [20-22] under these conditions degradation becomes independent of light intensity.

The influence of initial dye concentration on the degradation of CR was studied by varying the concentration from 1-10 *ppm*. The degradation of the dye over a concentration range from 1-10 *ppm* is shown in Figure 8. It is noted that as the dye concentration increases from 1-10 *ppm*, the degradation after continuous illumination reduces from 0.128 to 0.01. At a fixed light intensity, the decrease in conversion of CR with an increase in dye concentration can be attributed to the greater amount of dye competing for degradation and/or the reduction in the light intensity that reaches the ZnO surface. At very high concentrations, much of the light is screened by the solution and fewer photons are able to reach the ZnO surface [23]. Thus, the generation of electron-hole pairs is greatly reduced and in turn, the dye degradation is reduced due to absence of oxidizing species.

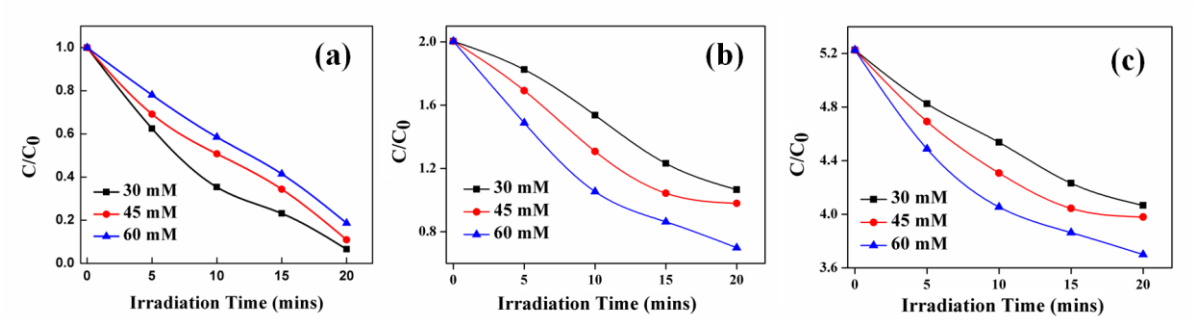

Figure 8. Photo degradation of CR under different concentrations of CR (a) 1 ppm, (b) 5 ppm (c) 10 ppm.

The effect of the amount of loading of photocatalyst on the decolourization of CR is shown in figure 9. .It clearly shows that the amount of photocatalyst affect the decolourization of the dyes.

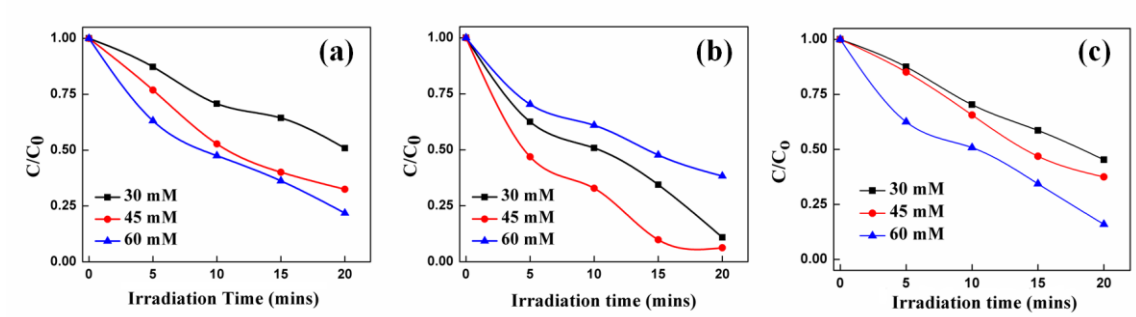

Figure 9. Photo degradation of CR under different amount of catalyst (a) 0.01 g, (b) 0.05g, (c) 1 g

It was observed that by increasing the amount of photocatalyst loading, the amount of decolourization also increased [24, 25]. This observation may be caused by the increase in the number of photons adsorbed on the photocatalyst or the number of activated molecules adsorbed on the photocatalyst surface with increase in amount of photocatalyst. At 50 mg photocatalyst leads the highest activity to a certain extent after that the catalyst shows the same activity like other catalyst loading degradation systems. After certain addition of catalyst the photo catalytic activity became in same rate [26, 27]. This is due to over loading of catalyst will not allow the light into the surfaces so that the reaction goes same speed after reaching the estimated amount.

IV. Conclusion

In this work, we have reported the synthesis of ZnO nanoparticles by simple chemical method. XRD analysis showed that the synthesized ZnO particle is in nanometer range. The SEM images show that the formation of spherical shaped nanoparticles and the agglomerations have been taken place. Absorption peak of the prepared sample is varied between 401-409 nm which is highly red shifted as compared to the bulk (360nm). The reflectance spectrum has less effect in scattering than absorption. The sudden decrease of reflectance at a particular wavelength, corresponding to the optical band gap means that the particles are almost uniformly distributed in the sample. Band gap energy of ZnO nanoparticle is varied between 3.04-3.1 eV. The photocatalytic activity results suggested that the as synthesized nanoparticles were exhibited enhanced photocatalytic efficiency for the sample prepared at 30 mM concentration. The effect of different operational

parameters were performed and the optimized condition for the effective photocatalytic degradation was achieved.

References

[1]. F. Dong, L. W. Wu, Y. J. Sun, M. Fu, Z. B. Wu, and S. C. Lee, J. Mater. Chem. *21*, (2011) 15171-15175.
[2]. H. J. Yan, Y. Chen, and S. M. Xu, Int. J. Hydrogen Energy *37*, (2012) 125.
[3]. P. S. Kumar, M. Selvakumar, S. G. Babu, S. Karuthapandian, and S. Chattopadhyay, Mater. Lett. *151*, (2015) 45-52.
[4]. P. S. Kumar, M. Selvakumar, S. G. Babu, S. K. Jaganathan, S. Karuthapandian, and S. Chattopadhyay, RSC Adv. 5, (2015) 57493-57499.
[5]. C. Richard, F. Bosquet, J.F. Pilichowski, J. Photochem. Photobiol. A: Chem. *108* (1997) 45.
[6]. M.D. Driessen, T.M. Miller, V.H. Grassian, J. Mol. Catal. A: Chem. *131* (1998) 149.
[7]. J. Villase_oor, P. Reyes, G.J. Pecchi, Chem. Technol. Biotechnol. *72* (1998) 105.
[8]. M.C. Yeber, J. Rodrıguez, J. Freer, N. Durian, H.D. Mansilla, Chemosphere *41* (2000) 1193.
[9]. V. Dijken, A.H. Janssen, M.H.P. Smitsmans, D. Vanmaekelbergh, K. Meijerink, Chem. Mater. *10* (1998) 3513.
[10]. S. Neppolian, B. Sakthivel, M. Arabindoo, V. Palanichamy, J. Murugesan, Environ. Sci. Health, Part A: Toxic/Hazard. Subst. Environ. Eng. *34 (9)* (1999) 1829.
[11]. Baruwati B, Kumar D K and Manorama S V. 2006. Sensors Actuators B 119 676.
[12]. Yadav A, Virendra Prasad, Kathe AA, Sheela Raj, Deepti Yadav, Sundaramoorthy Vigneshwaran N. Bulletin of Material Science (2006) *29:*641- 645
[13]. Klug H P and Alexander L E. X-ray diffraction Procedures for polycrystalline and Amorphous Materials, 1st edn, chapter 9, Wiley, New York, 1954
[14]. D. Lin, H. Wu, W. Zhang, He. Li, W. Pan, Appl. Phys. Lett. *94* (2009) 172103.
[15]. E. Neshataeva, T. Kümmell, G. Bacher, A. Ebbers, Appl. Phys. Lett. *94* (2009) 091115.
[16]. S. Lee, Y. Jeong, S. Jeong, J. Lee, M. Jeon, J. Moon, Superlatt. Microstruc. *44* (2008) 761.
[17]. P.S. Kumar, S.L. Prabavathi, P. Indurani, S. Karuthapandian, V. Muthuraj, Light assisted synthesis of hierarchically structured Cu/CdS nanorods with superior photocatalytic activity, stability and photocatalytic mechanism, Sep. Purif. Technol, *172* (2017) 192–201.
[18]. P. Latha, R. Dhanabackialakshmi, P.S. Kumar, S. Karuthapandian, Synergistic effects of trouble free and 100% recoverable CeO2/Nylon nanocomposite thin film for the photocatalytic degradation of organic contaminants, Sep. Purif. Technol. *168*, (2016) 124-130.
[19]. P.S. Kumar, S. Karuthapandian, M. Umadevi, A. Elangovan, V. Muthuraj, Light induced synthesis and synergistic effects of Sr/CdSe nanocomposite on the photodegradation of methylene blue dye solution, Mater. Focus 2016, *5*, 128–136.
[20]. K. Saravanakumar, P.S. Kumar, J.V. Kumar, S. Karuthapandian, R. Philip, V. Muthuraj, Controlled Synthesis of Plate Like Structured MoO_3 and Visible Light Induced Degradation of Rhodamine B Dye Solution, *Energy and Environment Focus* 5 (2016) 50–57.
[21]. S.G. Babu, R. Vinoth, D.P. Kumar, M.V. Shankar, H.L. Chou, K. Vinodgopal, B. Neppolian, Influence of electron storing, transferring and shuttling assets of reduced graphene oxide at the interfacial copper doped TiO_2 p-n hetero-junction for the increased hydrogen production, Nanoscale *7*, (2015) 7849–7857.
[22]. P.S. Kumar, M. Selvakumar, S.G. Babu, S. Induja, S. Karuthapandian, CuO/ZnO nanorods: An affordable efficient p-n heterojunction and morphology dependent photocatalytic activity against organic contaminants, J. Alloy Compd, *701* (2017) 562–573.
[23]. C. Karunakaran**,** S. Senthilvelan, S. Karuthapandian, Solar photooxidation of aniline on ZnO surfaces, Sol. Energy Mater. Sol. Cell. *89* (2005) 391−402.
[24]. P. Karthik, R. Vinoth, S.G. Babu, M. Wen, T. Kamegawa, H. Yamashita, B. Neppolian, Synthesis of highly visible light active TiO_2-2-naphthol surface complex and its application in photocatalytic chromium (VI) reduction, RSC Adv. *5* (2015) 39752-39759.
[25]. S.G. Babu, R. Vinoth, P.S. Narayana, D. Bahnemann, B. Neppolian, Reduced graphene oxide wrapped Cu_2O supported on C_3N_4: An efficient visible light responsive semiconductor photocatalyst, APL Mater. 3 (2015) 104415 (1-9)
[26]. P.S. Kumar, S. Sobiya, M. Selvakumar, S.G. Babu, S. Karuthapandian, Hierarchically structured CuO/g-C_3N_4 heterogeneous semiconductor photocatalyst with improved photocatalytic activity and stability, *Energy and Environment Focus*, 5 (2016) 139–149
[27]. H.Y. Chen, L.G. Qiu, J.D. Xiao, S. Ye, X. Jiang, Y.P. Yuan, Inorganic–organic hybrid NiO–g-C_3N_4 photocatalyst for efficient methylene blue degradation using visible light, RSC Adv., *4* (2014) 22491–22496.

International Journal of Engineering Science Invention (IJESI) is UGC approved Journal with Sl. No. 3822, Journal no. 43302.

T. Jeyapaul "An Efficient and Enhanced Photo catalytic Activity of Zno Nan particles on Mineralization of Congo red Dye in Aqueous Medium" International Journal of Engineering Science Invention (IJESI), vol. 07, no. 03, 2018, pp 12-18.